ELSEVIER

Thermochimica Acta 312 (1998) 33–45

thermochimica acta

Microcalorimetric and spectroscopic studies of the acidic- and physisorption characteristics of MCM-41 and zeolites

J. Jänchen[a,*], H. Stach[a], M. Busio[b], J.H.M.C. van Wolput[b]

[a] *ZeoSys (Zeolithsysteme), Haus 2.3, Rudower Chaussee 5, D-12484 Berlin, Germany*
[b] *Schuit Institute of Catalysis, Eindhoven University of Technology, P.O. Box 513, 5600 MB Eindhoven, The Netherlands*

Abstract

The acidic and sorption properties of Al containing MCM-41 molecular sieves in comparison with relevant FAU and MFI zeolites were investigated by *n*-hexane, benzene, acetonitrile, and water adsorption by means of microcalorimetry, isotherm measurements as well as FTIR and ^{1}H MAS NMR techniques, using acetonitrile or chloro-acetonitrile as probes. MCM-41 shows relatively weak Brønsted acidity, comparable with the LF proton of HY. The strongest sites are Lewis centres according to the strongest heats of adsorption and the corresponding characteristic CN frequencies of acetonitrile in contrast to the HY or the dealuminated form of HY. MCM-41 shows a physisorption behaviour of a well-defined mesoporous molecular sieve, which makes it favourable as a model substance. Whereas, the heats of adsorption of acetonitrile are mainly influenced by a specific interaction on the acidic sites in the meso- and microporous molecular sieves, the adsorption heat of a non-polar molecule like *n*-hexane is determined by the pore size or density of those materials. However, a pore-size effect on the adsorption heats of acetonitrile in acidic molecular sieves has to be taken into account while employing those heats as a measure of acidic strength. The contribution of the pore size governed dispersion interaction in MCM-41 is ca. 15 kJ/mol smaller than that in the narrow channels of MFI. © 1998 Elsevier Science B.V.

Keywords: Acidity; Adsorption; FTIR; ^{1}H MAS NMR; MCM-41; Microcalorimetry; Zeolites

1. Introduction

The influence of the molecular sieve composition and lattice structure on the acidic strength of bridging protons and adsorption properties of those molecular sieves is of obvious importance in acid catalysed reactions. Not only the number, kind and strength of the active sites but also the size of the pores, hosting the catalytically active sites, determine the catalytic activity. Significant progress has been made, using different physico-chemical methods [1], to determine the relationships based on different theoretical approaches.

Adsorption calorimetry combined with spectroscopy, such as Fourier Transform Infrared (FTIR) or nuclear magnetic resonance (NMR), using an adsorbed base as probe, is a powerful method for the characterisation of zeolites and molecular sieves as catalysts. A general statement concerning the importance of sorbate–catalyst interaction in defining catalytic activity was recently made in Ref. [2]. In Refs. [3–6] again the importance of studying catalyst–sorbate interaction in magic angle spinning nuclear magnetic resonance (MAS NMR) was emphasised. The principle of following the response of the hydroxyl groups to their interaction with adsorbed weak bases to determine the acidic strength, using IR is already well established [7,8] and applied by other

*Corresponding author.

0040-6031/98/$19.00 © 1998 Elsevier Science B.V. All rights reserved
PII S0040-6031(97)00438-3

groups [9]. Whereas spectroscopy gives information about the kind of acidic sites, microcalorimetry allows the determination of the number and strength by 'titration' of the sites with probe molecules like acetonitrile, ammonia, pyridine or alkylamines [10–16]. In one recent example (12b) the heats of adsorption of the latter have been correlated additionally with the gas-phase proton affinities of the probes. A combination of both microcalorimetry and spectroscopy, using a weak base without proton transfer, gives significant information about the properties of zeolites and molecular sieves as catalysts.

Recently, the pore size of molecular sieves has been extended towards uniform mesopores by the synthesis of a new family of ordered mesoporous materials [17]. One member of this family is MCM-41, which exhibits a hexagonal array of uniform mesopores in the range 1.5–10 nm. Because of the very narrow pore size distribution of a particular MCM-41 material and the possibility of incorporating Al into the SiO_2 framework with the creation of acidic sites [18], MCM-41 is a good model substance to extend our studies on microporous catalysts towards mesoporous molecular sieves [6,15].

We prepared and characterised a series of typical MCM-41 samples with a pore diameter of approximately 3 nm and with varying Si/Al ratios. In previous publications [19,20] we reported about the preparation, Al incorporation and first characterisation by XRD, TPD, FTIR, and ^{27}Al MAS NMR. In this paper, we present results of detailed adsorption experiments and spectroscopic studies on two MCM-41 samples in comparison to relevant MFI and FAU zeolites probing important catalytic properties such as the concentration and nature of the acidic sites as well as the pore-size effects on the specific- and physisorption properties of probe molecules and reactants.

2. Experimental

The MCM-41 samples were synthesised in static teflon coated autoclaves at 383 K for seven days. The reaction mixtures were prepared from varying amounts of sodium aluminate dissolved in tetramethylammoniumhydroxide, colloidal silica (LUDOX HS-40) and hexadecyltrimethylammonium chloride solution as liquid crystal templating agent. The silica faujasite (SiO_2FAU, Si/Al=95) was prepared by a thermochemical dealumination method [21] from the parent HY zeolite (Si/Al=2.4, ion-exchange degree 85%, the rest is Na) and used in this study. Silicalite (SiO_2MFI) was synthesised hydrothermally using tetrapropylammonium hydroxide. The specific pore volumes of the samples, given in Table 1 (column 4), and the X-ray powder diffraction patterns confirmed good quality and purity of the samples.

The differential molar heats of adsorption and isotherms were measured using a Calvet-type microcalorimeter (SETARAM C 80) at 303 K which was connected to a standard volumetric adsorption apparatus with MKS Baratron pressure sensors. Additional isotherms were measured gravimetrically using a McBain balance at 293 K. Before application, the samples were calcined in high vacuum ($<10^{-5}$ torr) at 673 K for 4–8 h.

IR spectra were measured at room temperature on a Bruker FTIR spectrometer IFS 113 v equipped with a vacuum cell. Self-supporting discs with a thickness of 7.5 mg/cm^2 were used. Activation of the samples was performed at 723 K in high vacuum for 1 h. After cooling down to room temperature the spectrum of the unloaded sample was taken, followed by adsorption of deuterated acetonitrile at an equilibrium pressure of ca. 0.9 torr for 30 min. Then again a spectrum was recorded. After this the loading of the samples were

Table 1
Some characteristic data of the samples used

Sample	Si/Al ratio	BET surface (m^2/g)	Specific pore volume (cm^3/g)	Pore diameter (nm)
MCM-41-25	25	1155	1.17	3
MCM-41-40	40	900	1.12	3
HY	2.4	—	0.31	1.12
SiO_2FAU	95	690 [b]	0.2 [a], 0.56 [b]	1.12 [a], 3 [b]
SiO_2MFI	∞	—	0.18	0.55

[a] Micropores.
[b] Mesopores.

reduced by lowering the equilibrium pressure to 0.04 torr and by desorption (30 min) at room temperature, 353 and 573 K, respectively, followed again by taking room temperature spectra after each step.

The ^{1}H MAS NMR measurements were performed at room temperature on a Bruker NMR spectrometer MSL 400 with a magnetic field of 9.4 T, the MAS spinning rate was 5–10 kHz. The samples for the NMR experiments were also degassed on a vacuum line at 723 K for 3–5 h in high vacuum. After cooling to room temperature, adsorption of CCl_3CN was carried out at equilibrium pressure of 0.9 torr and room temperature. After adsorption the samples were kept in a sealed tube. Prior to the NMR experiment, the samples were transferred into closed rotors (standard 4 mm rotors) in a glove box.

3. Results and discussion

3.1. Characterisation

Table 1 lists some characteristic data for the samples discussed here, evaluated from adsorption measurements. Whereas the texture data of the samples came from standard nitrogen adsorption measurements, the Si/Al ratios of the MCM-41 were estimated by chemical analysis [19] (bulk phase). However, according to ^{27}Al MAS NMR [19], for the MCM-41 samples only a small amount of non-framework Al exists. The Si/Al ratios of the zeolites (except SiO_2MFI) have been obtained by ^{29}Si MAS NMR (lattice values). As can be seen from the texture data, the SiO_2FAU has mesopores beside the 'zeolite pores'. The mesopores stem from the hydrothermal dealumination procedure [21]. Their pore diameter is of the order of MCM-41 pores, but the pore size distribution is much broader than found for MCM-41. The specific pore volume of the MCM-41 is ca. 50% higher than that of the silica faujasite.

Fig. 1. shows the FTIR spectra of the calcined (a) SiO_2FAU and (b) SiO_2MFI samples. According to the Si/Al ratios, given in the table, no bands for acidic protons can be found in the spectrum of the silica MFI. Only a small band, at 3744 cm^{-1}, appears in the OH stretching region due to some terminal SiOH groups. On the contrary, the strongly dealuminated FAU reveals a huge band at 3739 wave numbers, typically in shape with common porous silica and is assigned to terminal silanols. The bands in the range 1500–2000 cm^{-1} are overtones and combination modes of the fundamental lattice vibrations. A very similar spectrum with just the same band in the OH stretching region, at 3749 cm^{-1}, was found for all calcined MCM-41 samples (not shown in the figure). In both the cases, a large amount of SiOH groups should be located on the inner surface of the mesoporous MCM-41 tubes and in the secondary pores of the dealuminated FAU. Whereas a very small amount of Al in the crystalline SiO_2FAU gives two small bands, the LF band at 3567 and the HF band at 3630 wave numbers – both very characteristic for the faujasite type zeolites – no band for the expected acidic sites in MCM-41 have been found. Obviously, the Brønsted bands of the dry amorphous MCM-41 become, as well known for classical amorphous silica–alumina, 'invisible' in the IR which is in good agreement with results in Ref. [22].

3.2. Physisorption properties of the molecular sieves

In the following, the physisorption properties of the MCM-41 samples in comparison to the silica zeolites will be discussed. Unlike polar molecules, *n*-hexane exhibits almost non-specific interaction with the surface of the MCM-41 channels or in the silica zeolite pores. Fig. 2. shows the normalised heat curves and Fig. 3 the isotherms of *n*-hexane adsorption on the SiO_2FAU and MCM-41-25. The heat curve of MCM-41 is, after some decrease at the beginning due to a small influence of the acidic sites (see later), a smooth curve. There is roughly no difference between the adsorption heat of the monolayer (up to $\Theta=0.46$, $a=2.8$ mmol/g) and the heat for the condensation of the hexane in the mesopores ($0.46<\Theta<1$, $2.8<a<6$ mmol/g). Interestingly, the heat of condensation of the confined *n*-hexane in the MCM-41 pores is distinctly higher than the heat of condensation of the free liquid. The heat curve of SiO_2FAU behaves differently. The differential molar heat of adsorption first increases with rising amount of adsorbed *n*-hexane molecules up to a maximum and then drops to the values close to those of the MCM-41. As was already shown, the maximum corresponds to the filling of the micropores. Since the distance between the sorbed molecules in the cavities reduces, by filling up with

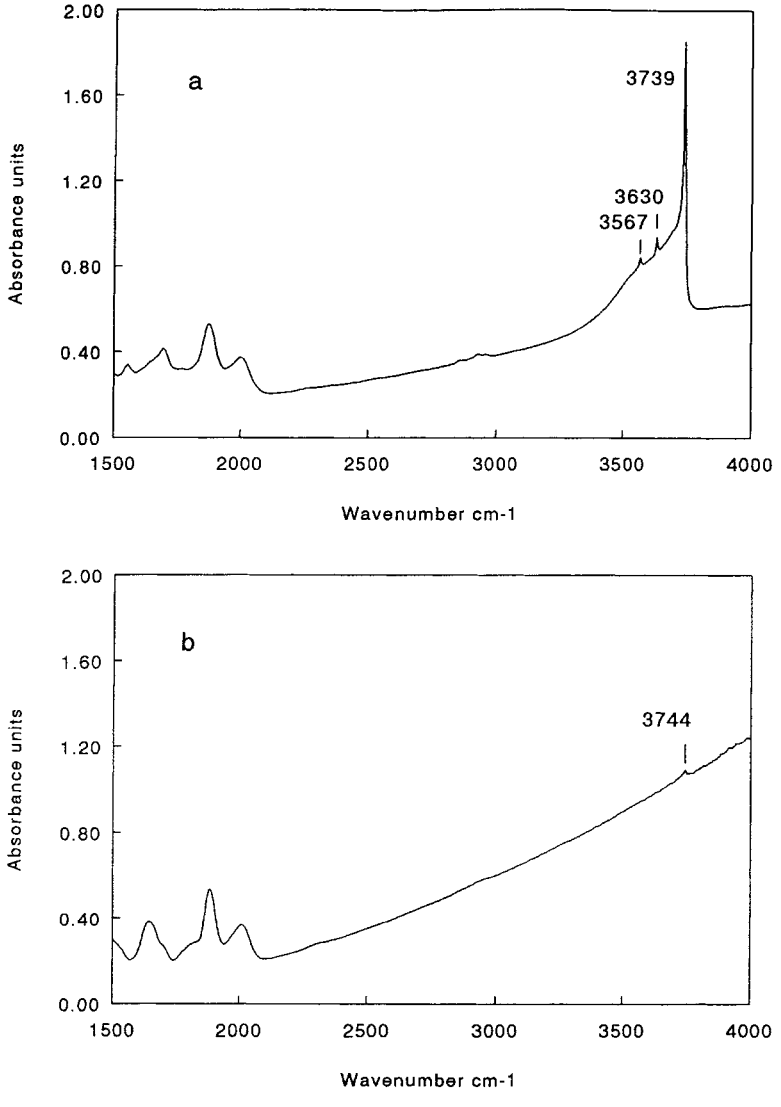

Fig. 1. FTIR spectra of the calcined (a) SiO_2FAU and the (b) SiO_2MFI.

n-hexane, the heat of adsorption increases by sorbate–sorbate interaction. The dropping part of the curve after the maximum is due to the beginning of adsorption in the smaller mesopores followed by filling of the 3 nm pores of the SiO_2FAU which are very close in diameter to the MCM-41 pores.

Recently published results of a pore-size effect in catalytic activity of the hydroisomerisation of *n*-hexane in zeolite catalyst with different pore diameters [23,24] have pointed out the significance of adsorption data in catalysis. It was shown that the heat of adsorption compensates parts of the activation energy. Consequently, the activity of the catalyst increases with decreasing pore diameter. Furthermore, the concentration of the reactant in the pores, at a given partial pressure, rises with decreasing pore size and influences the catalytic activity. Thus, the information about the adsorption equilibrium of the reactants is important for the interpretation of catalytic activity. This information can be found in Fig. 3, presenting the isotherms. It can be seen that at low equilibrium pressure of the *n*-hexane, the SiO_2FAU adsorbs more

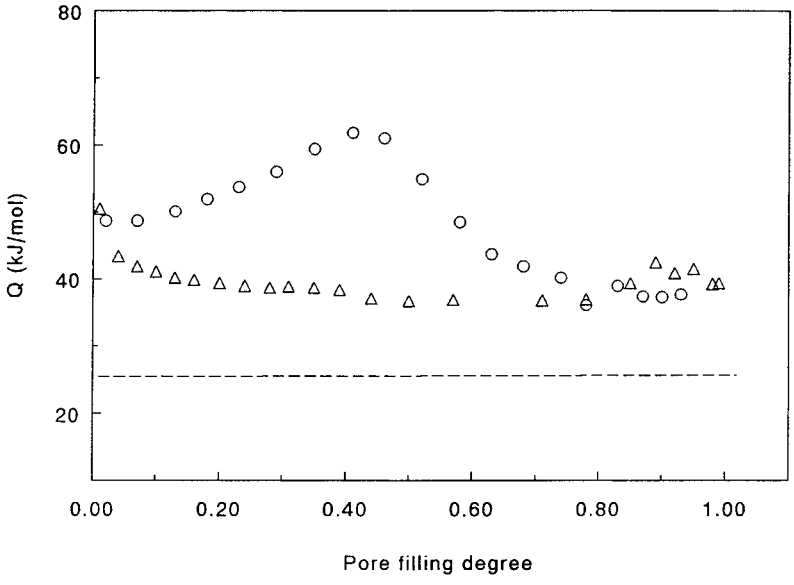

Fig. 2. Differential molar heats of adsorption of *n*-hexane at 303 K on MCM-41-25 (△) and SiO_2FAU (○) as function of the pore filling degree, dashed line denotes heat of condensation.

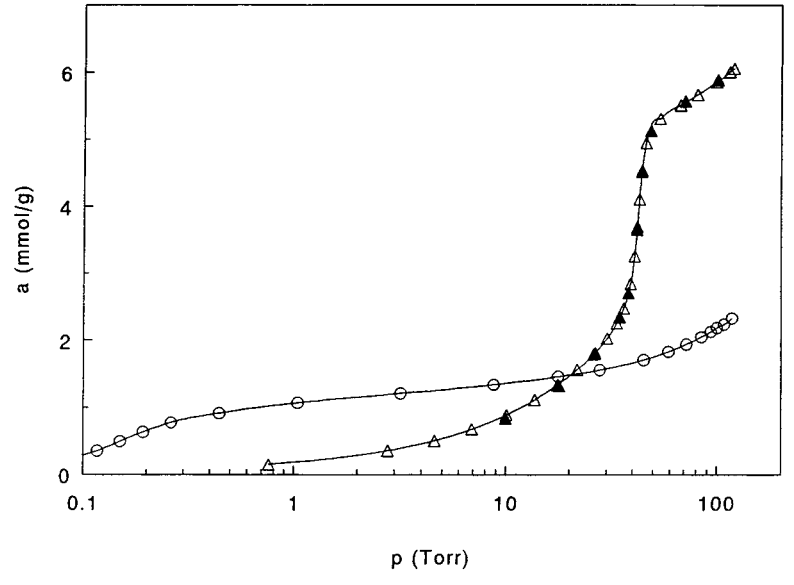

Fig. 3. Adsorption isotherms at 303 K of *n*-hexane on MCM-41-25 (△) and SiO_2FAU (○).

n-paraffin than MCM-41. It is because of the narrow pore diameter of the faujasite cavities. They are already filled at approximately 20 torr. Even at this pressure the monolayer in the MCM-41 channels is not complete (2.8 mmol/g), ca. 40 torr of pressure is needed to completely cover the inner surface of the tubes. The monolayer adsorption is followed by capillary condensation as indicated by a sharp rise in the isotherm within a very limited pressure range resulting from the narrow pore size distribution. The last, nearly

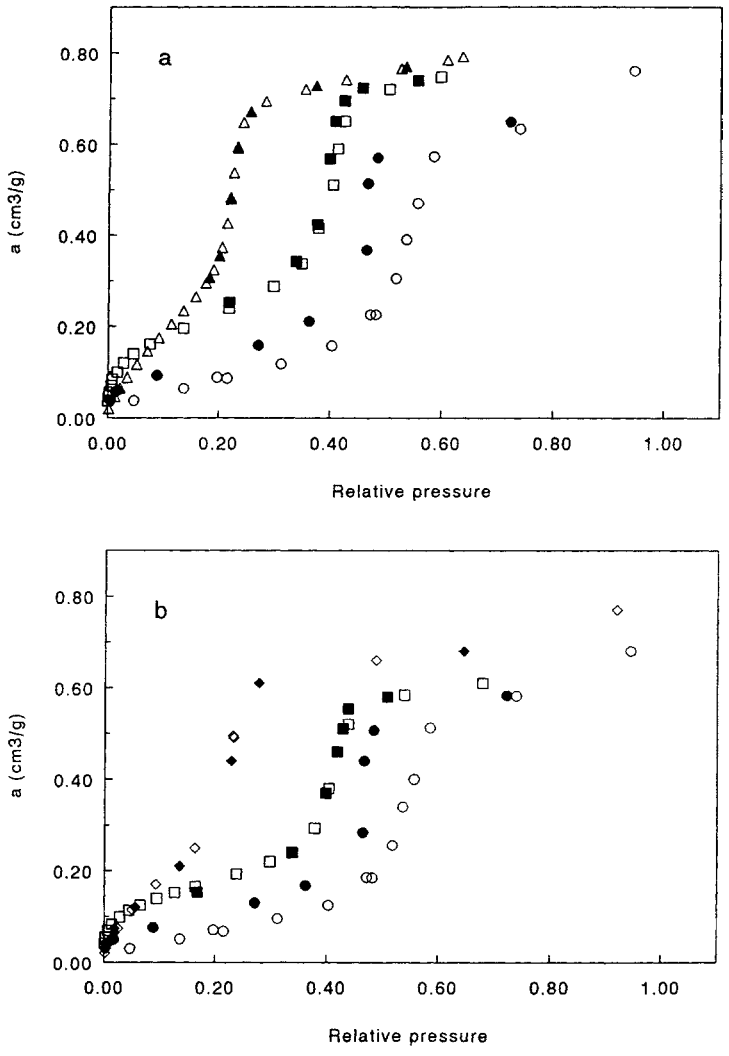

Fig. 4. Adsorption isotherms of *n*-hexane (△), (◇) benzene, acetonitrile (□) and water (○) on MCM-41-25, filled symbols denote desorption.

linear, part of the MCM-41 isotherm is, as suggested in Ref. [23], due to the adsorption on the outer surface of the very small MCM-41 particles and in their inter particular voids. Capillary condensation also takes place in the mesopores of SiO_2FAU. However, because of the less defined pore diameters and the smaller pore volume, the isotherm looks different in shape at pressure >40 torr as compared to the MCM-41.

Fig. 4a compares the *n*-hexane isotherm of MCM-41-25 with those of acetonitrile and water. The isotherms of benzene, acetonitrile and water on MCM-41-40 (Fig. 4b) exhibit a very similar behaviour. All isotherms, of both the samples (except for water), are of type IV according to the IUPAC classification with a very steep increase at a certain relative pressure which corresponds, based on the Kelvin equation, with a quite narrow pore size distribution as already shown before. According to the differences in surface tension and the molecular volume of the adsorbates, the capillary condensation takes place at varying relative pressures for the same pore diameter. The specific adsorption capacity for water is somewhat lower than the other above mentioned molecules.

Table 2
Pore structure parameters of (a) MCM-41-25 and (b) MCM-41-40 evaluated from adsorption isotherms of different molecules

Molecule	Specific pore volume at p/p_s=0.6, (cm^3/g)		BET surface area (m^2/g)		Kelvin diameter (nm)		Approx. pore diameter (nm)	
	(a)	(b)	(a)	(b)	(a)	(b)	(a)	(b)
Benzene	0.8	0.69	1050	860	2.66	2.66	3.4	3.4
n-Hexane	0.8	—	900	—	2.48	—	3.3	—
Acetonitrile	0.75	0.6	(625) [b]	(500) [b]	2.68	2.68	3.5	3.5
Water	0.72 [a]	0.6 [a]	(300) [b]	(270) [b]	2.8	2.8	3.3	3.3

[a] at p/p_s=0.8.
[b] Formal application of the BET equation.

The water isotherms are of type V and, in accordance with [25,26], they are not at all reversible. In contrast to this small polar molecule, the isotherms of nitrogen, benzene and *n*-hexane are completely reversible, and in the case of acetonitrile almost reversible (notice that the acetonitrile isotherm of the sample with the higher Si/Al ratio is reversible). Missing hysteresis loops are quite unusual for mesoporous materials. At present, this phenomenon is a point of controversy in the literature [27,28]. Previously reported adsorption isotherms of N_2, O_2, Ar and cyclopentane on MCM-41 [27,29] showed that the presence and size of the hysteresis loop depend on the adsorption, pore size and temperature.

Table 2 summarises some texture data of MCM-41-25 and MCM-41-40 evaluated from the above discussed adsorption isotherms. The pore volumes (second column of Table 2) differ slightly from the values calculated for nitrogen (1.07 or 0.93 cm^3/g at p/p_s=0.6, respectively), whereas all other sorbates in Table 2 reveal very comparable values for each sample. The application of the BET equation to the adsorption of the non-polar molecules, benzene and *n*-hexane (next column), gives realistic values whereas this equation fails in case of polar molecules. This is in accordance with the results of the microcalorimetric measurements (see later), indicating strong specific interaction of acetonitrile and water with the acidic sites and the silanol groups. Consequently, the inner surface of the pores is only partially covered by acetonitrile and water due to the hydrophobic character of the MCM-41 surface. The last two columns list the Kelvin diameter and based on it is an approximation of the pore diameter of the MCM-41 samples. The thickness of the adsorption layers was approximated by the diameter of the adsorbate molecules (benzene 0.37, *n*-hexane 4.3, acetonitrile 0.4 and water 0.26 nm). As can be seen, this method gives realistic values also in comparison to the 4 nm *d* spacing of the (100) reflection of the MCM-41 [19].

3.3. Specific sorption and spectroscopy

The specific interaction of acetonitrile on the acidic sites, as just mentioned, permits quantification of site types using characteristic heats of adsorption. Fig. 5 shows the differential heats of adsorption of acetonitrile on HY, SiO_2FAU and MCM-41-25. The heat curve of HY decreases continuously from ca. 80 to 65 kJ/mol up to a loading of 3.5 mmol/g which approximately equals the amount of stronger Brønsted sites (5 protons out of 6 protons and 1 Na per large cavity) of this sample. Corresponding values of heats for the interaction of acetonitrile with silanol groups on silica are $\leq$60 kJ/mol [30]. Consequently, the amount of 'Brønsted bonded' acetonitrile should be found in between the given heat interval. Since SiO_2-FAU is strongly dealuminated and leached by nitric acid, only a few strong acid sites, according to the Al concentration of ca. 0.2 mmol/g, can be expected. The strongly decreasing heat curve at very low loadings (up to 0.2 mmol/g), followed by a step from 0.2 to 1.2 mmol/g for the terminal SiOH, confirms this expectation. However, the higher starting level (70 kJ/mol) of this step indicates that some of the silanols are more acidic than silanols of common silica. This may be related to the structural defects in the mesopores of SiOH.

The heat curve of MCM-41-25 drops sharply from low to higher coverage until an inflection point near 60 kJ/mol is reached. The adsorbed amount of acetonitrile at this point is ca. 0.8 mmol/g which is close to

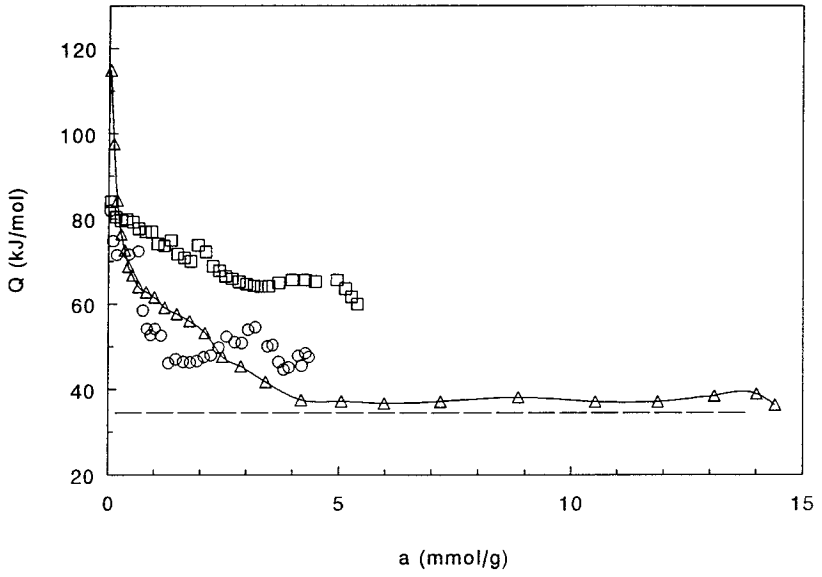

Fig. 5. Differential molar heats of adsorption of acetonitrile at 303 K on MCM-41-25 (△), zeolite HY (□) and SiO_2FAU (○), dashed line denotes the heat of condensation of acetonitrile.

the concentration of Al (0.7 mmol/g) in MCM-41-25. The corresponding values for MCM-41-40 are 0.4 mmol/g Al and 0.5 mmol/g acetonitrile (not shown in the figure). The presence of small amount of acetonitrile (0.2 mmol/g), at the very beginning of the heat curve with Q>80 kJ/mol, should be due to the molecules adsorbed on (Al based) strong Lewis sites. This Al is perhaps a framework or non-framework material. Finally, the step in the heat curve from 60 to 40 kJ/mol could be due to the interaction of acetonitrile with a huge amount of silanol groups. However, this presumption has to be verified by spectroscopic results. The remaining part of the CH_3CN is physisorbed in the MCM-41 pores, indicated by the low and constant heat of adsorption, which differs only a few kJ/mol from the heat of condensation of this molecule (dashed line in Fig. 5). This is in contrast to the situation of the non-polar *n*-hexane (Fig. 2).

Fig. 6 shows the isotherms of acetonitrile on the same samples. The shape of the isotherms of the high silica molecular sieves SiO_2FAU and MCM-41-25 are like the hexane isotherms due to their pore structure. Incorporation of Al into the faujasite structure enhances the concentration of Brønsted sites, and as a result, in analog to the heat curve, much more acetonitrile is adsorbed at low equilibrium pressure compared to the other two samples. The FTIR experiments were performed at loadings which can be taken from this figure at 0.9 and 0.04 torr. Even lower loadings have been achieved by desorption as described in Section 2.

Table 3 summarises the results of the FTIR measurements with acetonitrile on MCM-41 and different zeolites. Fig. 7 gives two examples of a set of different FTIR spectra in the CN stretching region obtained upon adsorption of decreasing amounts of deuterated acetonitrile. A comparable set of those FTIR spectra for MCM-41-25 is given in Ref. [19]. Acetonitrile can help in distinguishing between different OH species, as well as between Brønsted and Lewis sites by showing characteristic shifts of the CN modes from

Table 3
Wave numbers of the CN stretching modes of acetonitrile upon adsorption at 0.9 torr at room temperature on MCM-41-25 and on zeolites

Sample	CN Wave number (cm^{-1})			
SiO_2-MFI	2266	2274	2283	—
SiO_2-FAU	—	2274	2302	(2325)
HY	2265	2275	2300	(2320)
MCM-41-25	—	2274	2290	2330

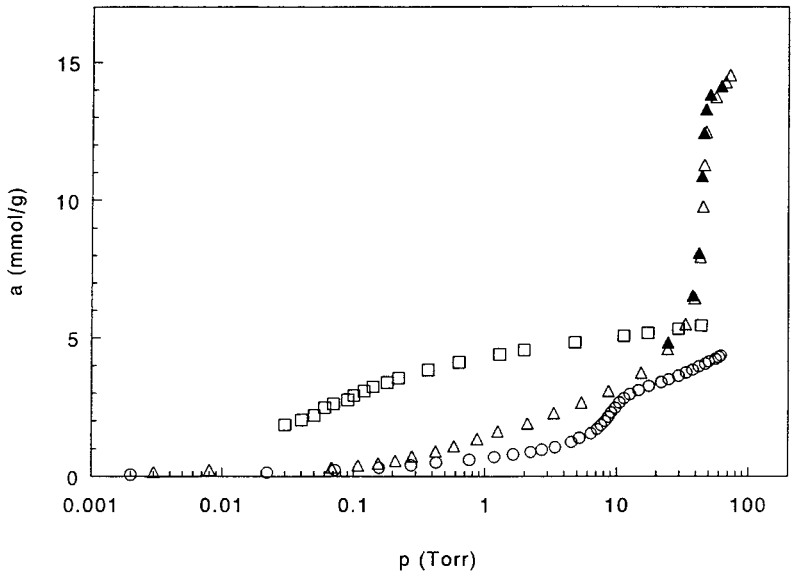

Fig. 6. Adsorption isotherms at 303 K of acetonitrile on MCM-41-25 (△), HY (□) and SiO_2FAU (○), filled symbols desorption.

2265 cm^{-1} for the physisorbed molecule to higher wave numbers for molecules adsorbed on different acidic sites [31].

Fig. 7(a) (SiO_2FAU) reveals three different CN bands (beside the stretching vibrations of the CD_3 group). The first CN mode (2274 cm^{-1}) is a characteristic of acetonitrile adsorbed on silanol groups, the second for Brønsted bonded acetonitrile (2320 cm^{-1}) and the third is due to the interaction on weak Lewis sites (2325 cm^{-1}). The latter was identified as five-coordinated Al, often found in non-framework Al of delauminated zeolites [31]. The strongest sites are the Brønsted centres. Since the silica MFI has a few silanol groups, the 2274 cm^{-1} band is small, and physisorbed acetonitrile appears in the first spectrum (0.9 torr, compare with 7a). The 'silanol band' is split for some reason into two bands. The acetonitrile is comparably strong bonded on those groups. All these wave numbers can be found in Table 3 for HY and MCM-41. As could be expected, HY exhibits all four kinds of sites, with the overwhelming majority being Brønsted centres, which are also the strongest. Thus, it can be concluded that the heat curve of HY in Fig. 5 represents interaction mainly on the stronger (up to 3.5 mmol/g) and weak Brønsted sites. Further, the part at the very beginning (up to 0.2 mmol/g) of the heat curve of the silica faujasite, after dealumination, is due to the remaining Brønsted centres (including some weak Lewis sites), and the following part, up to 1.2 mmol/g, depicts interaction on the silanols which should be located mainly in the mesopores.

The IR spectra of the calcined MCM-41 samples show, in the OH stretching region, a typical strong band for terminal silanol groups at 3749 cm^{-1} only, as already discussed. However, after adsorption of acetonitrile at ca. 0.9 torr equilibrium pressure (corresponds to ca. 2 mmol/g), two bands at 2274 cm^{-1} with a shoulder at 2290 and 2330 cm^{-1} appear due to the CN stretch (see Table 3). The first mode is again characteristic for acetonitrile adsorbed on silanol groups and the second for the strong Lewis bonded base. The shoulder at 2290 cm^{-1} is typical of acetonitrile adsorbed on weak Brønsted sites [15]. Step by step desorption reveals that the band at 2274 cm^{-1} disappears first, leaving a small band at 2290 cm^{-1} (Brønsted bonded) and a stronger band at 2330 cm^{-1} due to the Lewis bonded acetonitrile. The latter one remains at a lower intensity, even after desorption at elevated temperature (573 K), indicating strong Lewis acidity which is perhaps caused by the interaction on threefold coordinated non-framework Al [31]. Thus, the first part of the heat curve up to ca. 0.7 mmol/g represents the specific adsorption on acidic sites, strong Lewis and weak Brønsted centres, and up to

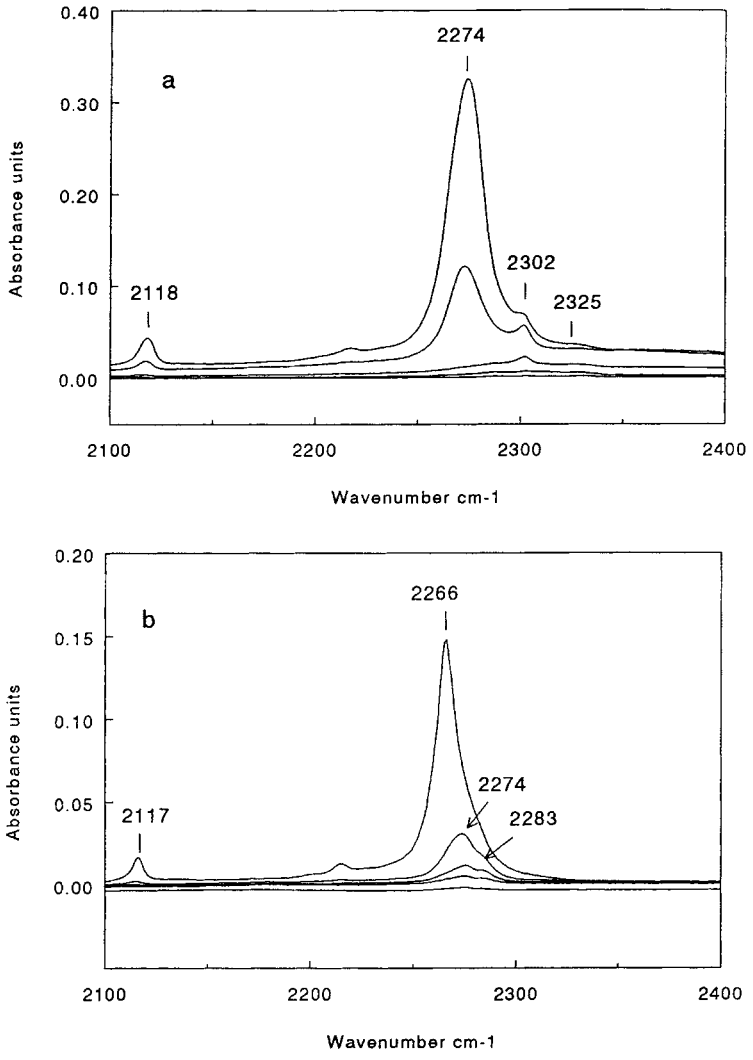

Fig. 7. Different spectra of CD_3CN adsorbed on (a) SiO_2FAU and (b) SiO_2MFI with decreasing loadings in the CN stretching region; spectra from top to bottom: equilibrium pressure 0.9 and 0.04 torr, after desorption at room temperature, at 353 and 573 K for 30 min.

4.5 mmol/g on the enormous amount of silanol groups.

Analogous to the FTIR spectra of the calcined MCM-41 samples, the ^{1}H MAS NMR spectrum of MCM-41-40 in Fig. 8 (trace a) shows only one strong signal at 1.9 ppm, characteristic of silanols. However, after the adsorption of a base, in this case chloroacetonitrile has no H-D exchange, potentially the stronger sites become visible (trace b). Table 4 presents the chemical shifts and extra shifts upon adsorption of MCM-41-40 compared to some zeolites. As can be seen, the extra shift for MCM-41 is low and not easy to estimate. The strongest sites, in MCM-41 seem to be comparable in strength with the LF proton of HY. Therefore, according to the FTIR, ^{1}H MAS NMR and the adsorption heats of acetonitrile, it can be concluded that weak Brønsted acidity dominates MCM-41 though the acidic OH are IR and NMR 'invisible' in the calcined form.

The difference in pore size between the MCM-41 and the microporous zeolites is considerable. Since some pore-size effects on the specific interaction of

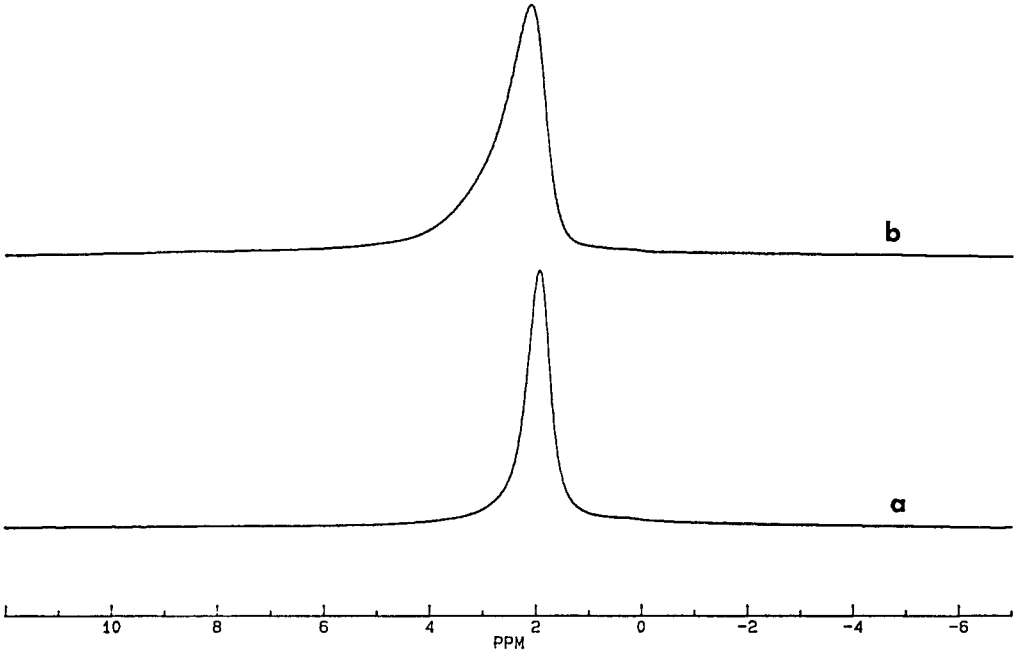

Fig. 8. ^{1}H MAS NMR spectra of MCM-41-40 (a) before adsorption and (b) upon adsorption of chloro-acetonitrile at 1 mbar and room temperature.

the probe molecule, in microcalorimetry, can be expected, the part of the overall dispersion interaction of acetonitrile will be estimated in the following. For this reason the heat curves of the silica MFI and the silica FAU are plotted in Fig. 9. A plateau-like part of the heat curves, indicated by dotted lines in the figure, should only represent the physisorption of acetonitrile in the micropores of those samples. In both the cases, the first decreasing part of the heat curve is due to the specific interaction, as shown in Fig. 7, and the increasing second half with the maximum is perhaps caused by sorbate–sorbate interaction because of the high concentration in the pores. The section in-between, extrapolated to zero-coverage, will be taken as a characteristic value for 'pure' dispersion interaction. The value for MCM-41 is taken from Fig. 5.

Table 4
^{1}H MAS NMR chemical shift differences upon adsorption of chloro-acetonitrile of MCM-41 and zeolites

Sample	δ_H before adsorption	δ_H after adsorption	$\Delta\delta_H$
H-MFI	4.1	9.0	4.9
HY (HF band)	4.1	8.5	4.4
(LF band)	4.7	7.7	3.0
MCM-41-40	1.9	2.1–5	0.2–3

In Fig. 10, these values are plotted as a function of the pore diameter together with the initial heats of *n*-hexane (for comparison) in SiO_2MFI, SiO_2FAU and MCM-41. Additional values of *n*-hexane adsorption on an SiO_2MOR (Si/Al=130) and a large pore silica are included [32]. The latter approximates an almost flat surface because of the large pore diameter of ca. 20 nm. As can be seen from the figure, the heat of adsorption of *n*-hexane drops by the factor of two from the silica zeolites with very narrow pores (0.55 nm) to a flat surface (20 nm pores). Acetonitrile reveals a similar but much less pronounced result. The heats of physisorption of the smaller acetonitrile molecule decrease by only 15 kJ/mol, changing the pore diameter from 0.55 to 3 nm. In Ref. [15], another example is given for the adsorption of acetonitrile in AEL of ca. 50 kJ/mol (AlPO-11, comparable in pore diameter with MFI) and AFI of ca. 40 kJ/mol (matches MOR in pore size). Here the difference amounts to 10 kJ/mol, and the given values fit quite well into the results of Fig. 10. Thus, a limited but a measurable contribution

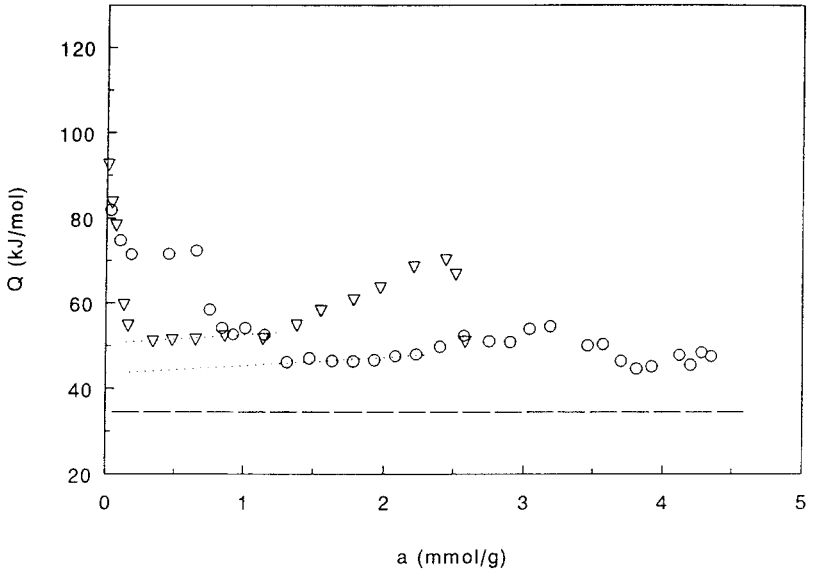

Fig. 9. Differential molar heats of adsorption of acetonitrile at 303 K on SiO_2FAU (○) and SiO_2MFI (▽), dashed line denotes the heat of condensation of acetonitrile.

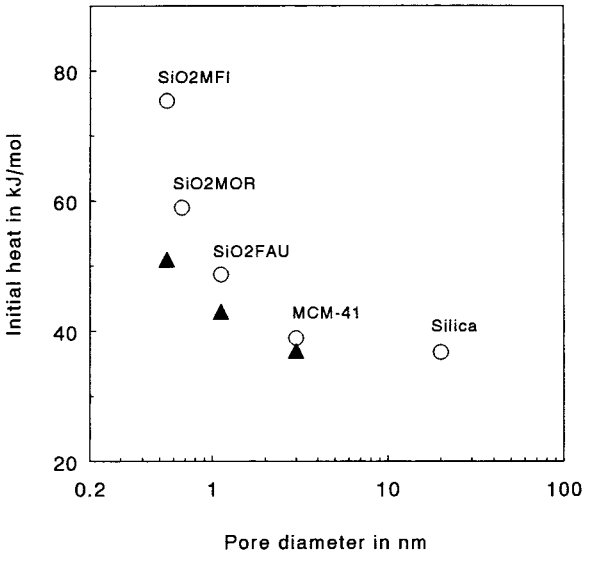

Fig. 10. Initial heats of adsorption of *n*-hexane (○) and physisorption heats of acetonitrile (▲) on silica molecular sieves as function of the pore diameter.

of dispersion interaction has to be taken into account before comparing heats of adsorption of bases as a measure of acidic strength for catalysts with large differences in their pore size.

4. Conclusions

Incorporation of Al into the MCM-41 network results in the formation of acidic sites such as weak Brønsted sites and some strong Lewis centres, as could be shown by a combined study of microcalorimetry, FTIR and ^{1}H MAS NMR with acetonitrile or chloroacetonitrile as probe, respectively. The concentration of both kinds of sites corresponds approximately with the amount of Al in the MCM-41 samples.

MCM-41 seems to be a unique model substance for adsorption studies in mesopores. The heats of adsorption of a non-polar molecule (*n*-hexane) perfectly fit into the dependence of the heats of adsorption on the pore diameter in zeolites and large mesopores as approximation of a flat surface. Influence of the pore size on the interaction of acetonitrile is less pronounced but has to be taken into account.

Acknowledgements

The kind support for this work by J.H.C. van Hooff (Eindhoven) and the helpful assistance in the measurements of the NMR spectra by J.W. de Haan and L.J.M. van de Ven are acknowledged.

References

[1] R.A. van Santen, G.J. Kramer, Chem. Rev. 95 (1995) 637.
[2] M. Bull, A.K. Cheetham, N.M. Powell, J.A. Ripmeester, C.I. Ratcliffe, J. Am. Chem. Soc. 117 (1995) 4328.
[3] J.F. Haw, M.B. Hall, A.E. Alvaro-Swaisgood, E.J. Munson, Z. Lin, L.W. Beck, T. Howard, J. Am. Chem. Soc. 116 (1994) 7308.
[4] D. Freude, Chem. Phys. Lett. 235 (1995) 69.
[5] H. Sachsenröder, E. Brunner, M. Koch, H. Pfeifer, B. Staudte, Micropor. Mater. 6 (1996) 341.
[6] J. Jänchen, J.H.M.C. van Wolput, L.J.M. van de Ven, J.W. de Haan, R.A. van Santen, Catal. Lett. 39 (1996) 147.
[7] V.B. Kazansky, Accounts Chem. res. 24 (1991) 379.
[8] E. Löffler, U. Lohse, Ch. Peuker, G. Öhlmann, L.M. Kustov, V.L. Zholobenko, V.B. Kazansky, Zeolites 10 (1990) 266.
[9] M.A. Makarova, A.F. Ojo, K. Karim, M. Hunger, J. Dwyer, J. Phys. Chem. 98 (1994) 3619.
[10] A. Auroux, Topics in Catalysis, in: G. Somorjai, J.M. Thomas (Eds.), 4 (1,2), 1997, pp. 71–89.
[11] I. Bankós, J. Valyon, G.I. Kapustin, D. Kallo, A.L. Klachko, T.R. Brueva, Zeolites 8 (1988) 189.
[12] (a) D.L. Parillo, R.J. Gorte, J. Phys. Chem. 97 (1993) 8786; (b) C. Lee, D.J. Parrillo, R.J. Gorte, W.E. Farneth, J. Am. Chem. Soc. 118 (1996) 3262.
[13] M.R. Gonzalez, S.B. Sharma, D.T. Chen, J.A. Dumesic, Catal. Lett. 18 (1993) 183.
[14] L.C. Jozefowicz, H.G. Karge, E.N. Coker, J. Phys. Chem. 98 (1994) 8053.
[15] J. Jänchen, M.P.J. Peeters, J.H.M.C. van Wolput, J.P. Wolthuizen, J.H.C. van Hooff, U. Lohse, J. Chem. Soc. Faraday Trans. 90 (1994) 1033.
[16] F. Eder, J.A. Lercher, J. Phys. Chem. B 101 (1997) 1273.
[17] C.T. Kresge, M.E. Leonowicz, W.J. Roth, J.C. Vartuli, J.S. Beck, Nature 359 (1992) 710.
[18] A. Corma, V. Fornés, M.T. Navarro, J. Pérez-Pariente, J. Catal. 148 (1994) 569.
[19] M. Busio, J. Jänchen, J.H.C. van Hooff, Microporous. Mater. 5 (1995) 211.
[20] J. Jänchen, M. Busio, M. Himtze, H. Stach, J.H.C. van hooff, in: H. Chon, S.K. Ihm, Y.S. Uh (Eds.), Stud. Surf. Sci. Catal., 105 (1997) 1731.
[21] U. Lohse, E. Alsdorf, H. Stach, Z. Anorg. Allgem. Chem. 447 (1978) 64 and H. Stach, U. Lohse, H. Thamm, W. Schirmer, Zeolites (1986) 74.
[22] F. Di Renzo, B. Chiche, F. Fajula, S. Viale, E. Garrone, in: J.W. Hightower, W.N. Delgass, E. Iglesia, A.T. Bell (Eds.), Stud. Surf. Sci. Catal. 101 (1996) 851.
[23] A. van der Runstraat, J.A. Kamp, P.J. Stobbelaar, J. van Grondelle, S. Krijnen, R.A. van Santen, J. Catal., 171 (1997) 77.
[24] E.G. Derouane, J.M. Andre, A.A. Lucas, J. Catal. 110 (1988) 58.
[25] T. Boger, R. Roeky, R. Gläser, S. Ernst, G. Eigenberger, J. Weitkamp, Microporous Mater. 8 (1997) 79.
[26] S. Inagaki, Y. Fukushima, K. Kuroda, J. Colloid Interface Sci. 180 (1996) 623.
[27] J. Rathouský, A. Zukal, O. Franke, G. Schulz-Ekloff, J. Chem. Soc. Faraday Trans., 90 (1994) 2821 and 91 (1995) 937.
[28] P.I. Ravikovitch, S.C.Ó. Domhaill, A.V. Neimark, F. Schüth, K.K. Unger, Langmuir 11 (1995) 4765.
[29] P.J. Branton, P.G. Hall, K.S.W. Sing, H. Reichert, F. Schüth, K.K. Unger, J. Chem. Soc. Faraday Trans. 90 (1994) 2965.
[30] B.V. Kuznetsov, N.A. Tuan, T.A. Rachmanova, Ads. Sci. Technol. 6 (1989) 27.
[31] A.G. Pelmenshikov, R.A. van Santen, J. Jänchen, E. Meijer, J. Phys. Chem. 97 (1993) 11071.
[32] J. Jänchen, H. Stach, L. Uytterhoeven, W.J. Mortier, J. Chys. Chem. 100 (1996) 12489.